Colloid and Interface Science Communications 28 (2019) 20–28

Contents lists available at ScienceDirect

Colloid and Interface Science Communications

journal homepage: www.elsevier.com/locate/colcom

Embedding CuO Nanoparticles in PDMS-SiO_2 Coating to Improve Antibacterial Characteristic and Corrosion Resistance

Shima Tavakoli[a], Shervin Nemati[b], Mahshid Kharaziha[a,*], Safoura Akbari-Alavijeh[c]

[a] Department of Materials Engineering, Isfahan University of Technology, Isfahan 84156-83111, Iran
[b] Department of Materials Science and Engineering, Sharif University of Technology, Azadi Avenue, P.O. Box 11155-9466, Tehran, Iran
[c] Department of Food Science and Technology, College of Agriculture, Isfahan University of Technology, Isfahan 84156-83111, Iran

ARTICLE INFO

Keywords:
Nanocomposite coating
Biocompatibility
CuO nanoparticles
Hydrophobicity
Antibacterial activity

ABSTRACT

The purpose of this paper was to develop the hydrophobic nanocomposite coatings of polydimethylsiloxane (PDMS)-SiO_2-CuO to improve biocompatibility, corrosion resistance and antibacterial property of 316 L stainless. In this research, after synthesize of CuO and SiO_2 nanopowders using wet-chemical approaches, PDMS-SiO_2-CuO coatings consisting of various amounts of CuO nanoparticles were developed using dip-coating process. The nanocomposite coatings were characterized with regard to the structural and physical properties, corrosion resistance, antibacterial activity and cellular interactive responses. The results showed that incorporation of CuO nanoparticles < 2 wt% improved the corrosion resistance of 316 L stainless steel. At higher CuO nanoparticle contents (> 1 wt%), the agglomeration of nanoparticles and their cytotoxic effects resulted in reduced antibacterial characteristics and MG63 cell viability and proliferation. In summary, PDMS-SiO_2-CuO nanocomposite coating with significant antibacterial and anticorrosion behavior could be a promising coating for biomedical implants.

1. Introduction

Metal alloys have been increasingly applied in surgical implants and devices [1]. Specifically, stainless steel 316 L has attracted many attentions for orthopedic implants due to its biocompatibility, corrosion resistance, low costs and availability [2,3]. However, in long-term applications, corrosion resistance of stainless steel 316 L could be attacked by aggressive biological environments [4]. Many studies, conducted in vitro and in vivo, confirm the toxic effects of ion releasing from stainless steel on the mouse epithelium, alternation in the cellular population of spleen and alternation of human lymphocyte-surface antigens [5,6]. Moreover, studies demonstrate that released ions from stainless steel 316 L could have undesirable effects on the proliferation and differentiation of osteoblasts [7]. In addition to weak corrosion resistivity, there are other important characteristics such as antibacterial activity and bacterial adhesion which could threat the function of metallic implants [8].

In order to overcome these issues, various types of polymeric (i.e. polycaprolacton (PCL) [9], chitosan [10] and polydimethylsiloxane (PDMS) [11]), ceramic (i.e. hydroxyapatite [3]) and nanocomposite (i.e. PCL-forsterite [12] and PCL-gelatin [13]) coatings have been developed on the metallic substrates. In this regard, PDMS has been introduced as a polymer with significant properties for various biomedical applications from diagnostics to therapeutics [14]. PDMS belongs to a group of organosilicon compounds which could endow hydrophobicity and in some cases super-hydrophobicity (water contact angle > 150°) to surface [15,16]. For instance, Tserepi et al. [17] developed super-hydrophobic PDMS film on Si substrates to control the surface geometrical characteristics and hydrophobicity. Moreover, incorporation of nanoparticles within PDMS coating could improve hydrophobicity and corrosion resistance. Silica nanopowder is one of the most promising corrosion inhibitors for stainless steel [18]. For instance, Vasconcelos et al. [19] demonstrated that chemical resistance of stainless steel improved with a silica coating. In addition, incorporation of silica to PDMS could improve the surface roughness, while it could mimic the surface morphology of self-cleaning plant leaves. This surface topology enhances water contact angel dramatically, leading to improved super-hydrophobicity property and reduction of corrosion rate [20,21]. Recently, Xie et al. [22] found that a PDMS/SiO_2 coating on the surface of magnesium alloys, could simultaneously improve hydrophobicity and anti-corrosion of surfaces. However, these nanocomposites did not show any antibacterial activity which is beneficial for biomedical implants.

Recent results revealed that, nanoparticulate silver, silicon, copper,

* Corresponding author.
E-mail address: kharaziha@cc.iut.ac.ir (M. Kharaziha).

https://doi.org/10.1016/j.colcom.2018.11.002
Received 11 October 2018; Received in revised form 3 November 2018; Accepted 5 November 2018

gold, zinc and their oxides affect the bacterial populations which could be helpful to improve antibacterial properties of various implants [23,24]. Among them, copper oxide nanoparticles (CuO-NPs) have been selected as promising candidates due to their antibacterial function, bacteria adhesion performance and specially, lower prices compared to noble metals with similar properties [23,25]. These kinds of ionic metal oxides might be exceptionally great antimicrobial agents as they can be prepared with extremely high surface areas and unusual crystal morphologies [26]. The results show that the antibacterial characteristic of CuO-NPs is due to the production of reactive oxygen species (ROS) from the nanoparticles which results in the oxidative damages to cell construct [27]. However, the microbial sensitivity to the CuO-NPs depends on the microbial species and also nanoparticle morphology. In this way, CuO-NPs with rod and platelet morphology shows more effective bacterial retardant behavior [28].

The objective of this study was to simultaneously improve antibacterial properties and corrosion resistance of stainless steel 316 L with innovative coating consisting of PDMS-SiO_2 and CuO components. Results of this study may provide a new strategy to gain effective antibacterial activities, and biocompatibility in medical implants and devices.

2. Materials and Methods

2.1. Sample Preparation

Austenitic stainless steel 316 L sheets with sizes of 1×1 cm^2 was used as the substrates. In order to neglect surface roughness behavior, the substrates were polished mirror like and ultrasonically cleaned in distilled water and acetone to wash out any contaminations. Subsequently, specimens were heat treated at 350 °C for 1 h and, consequently, cooled in electrical furnace to obtain oxide layer. Finally, the samples were treated in H_2SO_4:H_2O_2 solution with molar ratio of 4:1 for 1 h to form $-OH$ groups.

2.2. Synthesis of CuO Nanoparticles

Green process was applied to synthesize CuO nanoparticles using *Aloe Vera* as a reducing agent (Fig. 1, step 1). Primarily, *Aloe Vera* extract was prepared by heating 25 g chopped leaves in 30 ml deionized (DI) water for 30 min at 110 °C. Then, the solution was passed through a Whatman filter paper to remove any solid particle. *Aloe Vera* extract was consequently added to the aqueous solution of copper precursor ($CuCl_2.2H_2O$, 0.6 mM), stirred at 110 °C for 30 min and then kept at 100 °C for 45 min in the electrical oven. After 72 h aging at room temperature, aqueous solution of 15 M NaOH was added to above solution until the color of mixture changed to brown. As prepared solution was centrifuged for 10 min and as-precipitated CuO-NPs were dried at room temperature.

2.3. Synthesize of Silica Nanoparticles

Silica nanoparticle was synthesized using sol-gel method, similar to the previous research [29]. Briefly, 0.5 ml tetraethyl orthosilicate (TEOS, Merck) and 0.5 ml methyl trichlorosilane (MTS, Merck) were added to 10 ml methanol and let them stir up to get homogenous mixture. Consequently, 0.1 M HCl was added to above solution and was stirred for 1 h to complete hydrolysis reaction. At last, 1 ml ammonium hydroxide (13 M NH_4OH, Merck) was added, under stirring, for condensation of silica sol. Afterwards, the sol was kept at room temperature for 24 h and dried at 80 °C for 1 h. Finally, the dried gel was calcined at 750 °C for 1 h.

2.4. Preparation of PDMS-SiO_2-CuO Nanocomposite Coating

Primarily, polydimethylsiloxane (PDMS, Sylgard® 184 Silicone Elastomer) solution with concentration of 50 wt% in toluene (Sigma-Aldrich) was prepared. After formation of a homogenous solution, silica nanoparticles with concentration of 20 wt% was added to above solution and stirred for 30 min. In the next stage, CuO nanoparticles with various concentrations of 0.5, 1 and 2 wt% was added to PDMS-SiO_2 suspension, separately. Followed by 30 min stirring and 30 min ultrasonication, curing agent of PDMS (PDMS: PDMS curing agent weight ratio = 10:1) was added and stirred for 10 min, before coating process.

To develop nanocomposite coating, the substrates were dipped at a 45° angle with the speed of 5 $^{mm}/_{s}$ and kept for 3 min. After withdrawing at the same speed, the samples were allowed to be dried for 5 min. The coating process was repeated for two times in order to enhance the coating's thickness. Finally, in order to cure the PDMS, the coated samples were annealed at 150 °C for 90 min. To distinguish the samples and for simplification, they were given abbreviation names; PDMS stands for pure PDMS coating, PS stands for PDMS-SiO_2, PSC0.5 stands for PDMS-SiO_2–0.5 wt% CuO, PSC1 stands for PDMS-SiO_2–1 wt% CuO and PSC2 stands for PDMS-SiO_2–2 wt% CuO.

2.5. Characterization of the Nanocomposite Coating

X-ray diffractometer, (XRD, X-pert, Philips) using Ni filtered Cu Kα (λ CuKα = 0.154186 nm, radiation at 40 kV and 30 mA) over the 2θ range of 30–80°, was employed to analyze phase structures. Fourier transform infrared spectroscopy (FTIR, Bomem) was also employed to establish the functional groups of the Silica nanoparticles and nanocomposite coatings. In addition, the morphology of the powders and coatings were considered by scanning electron microscopy (SEM

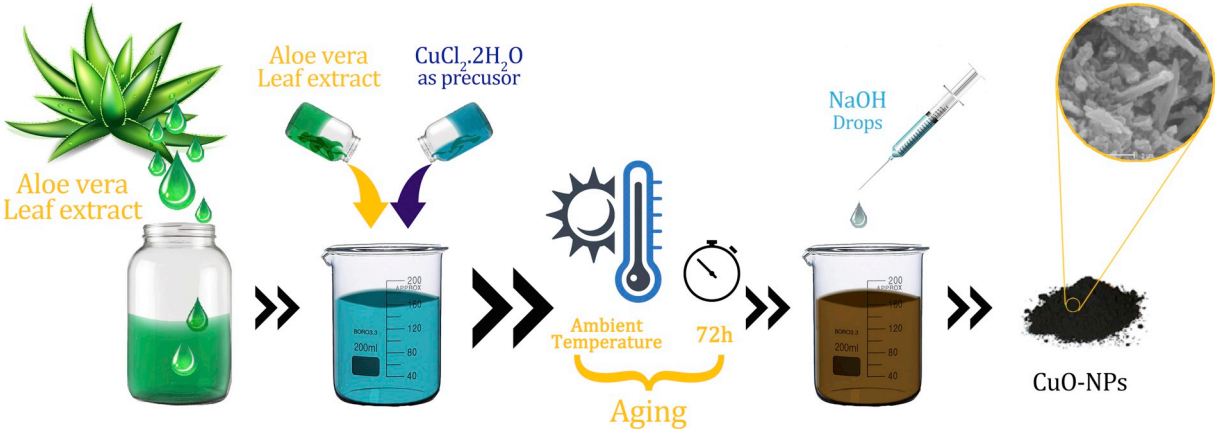

Fig. 1. Schematic diagram describing the synthesize process of CuO nanoparticles.

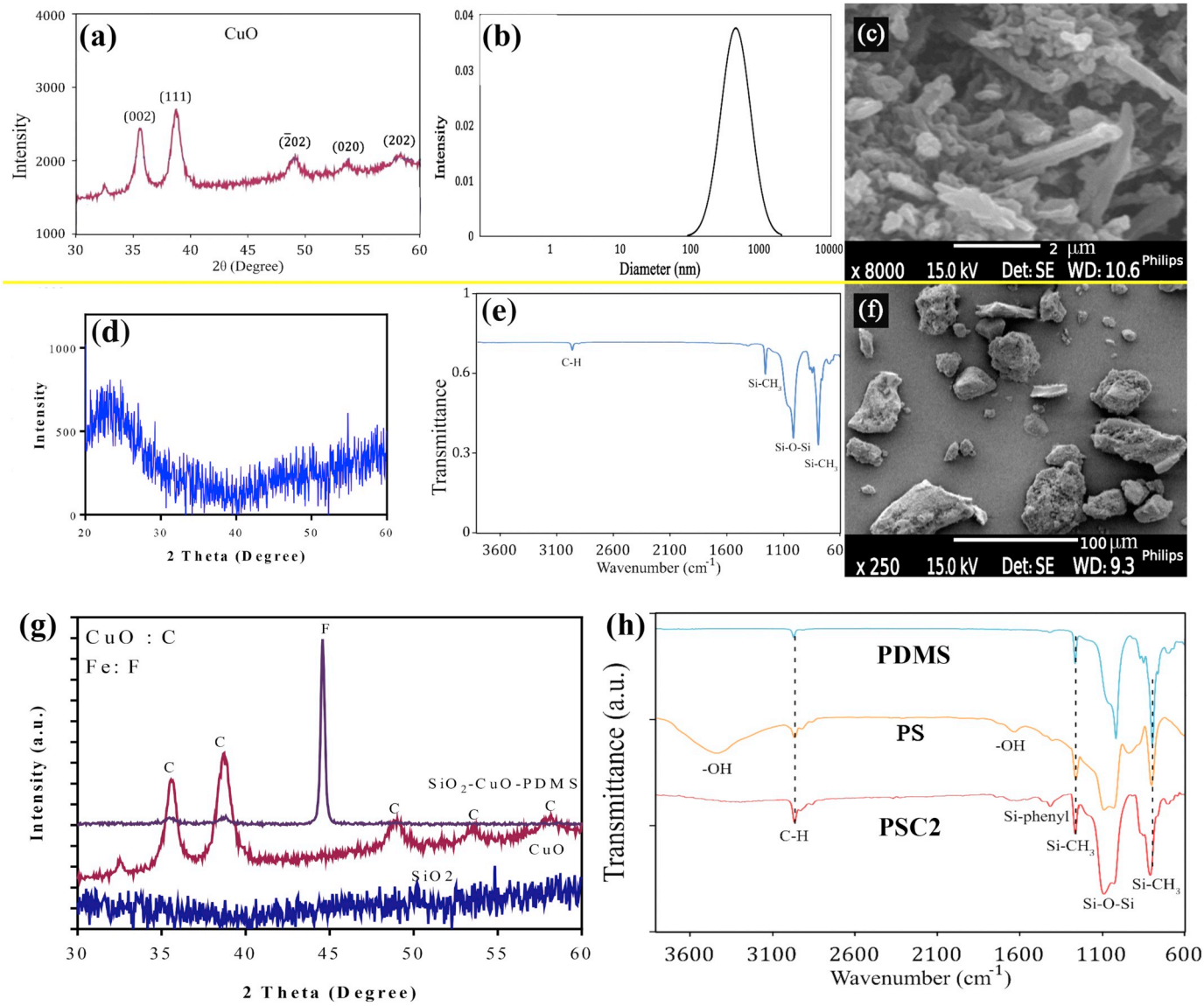

Fig. 2. Characterization of CuO and silica nanoparticles as well as nanocomposite coatings: a) XRD pattern, b) DLS diagram and c) SEM image of CuO-NPs. d) XRD pattern, e) FTIR spectrum and f) SEM image of silica nanopowders. g) XRD patterns and h) FTIR spectra of PDMS, PDMS-SiO_2 (PS) and PDMS-SiO_2–2 wt% CuO (PSC2) coatings.

Phillips XL 30: Eindhoven, The Netherlands). Before imaging, the samples were gold-coated. Moreover, the dispersion of CuO and SiO_2 nanoparticles within the coatings was analyzed by SEM-EDS (Scanning Electron Microscopy-Energy Dispersive Spectroscopy) element mapping. In addition, the particle size distribution of CuO nanopowder was also estimated using dynamic light scattering (DLS) technique.

In order to measure surface roughness based on ISO 1997 standard, laser surface profilometer (Mitutoyo) was used and the roughness value (Ra) was determined. In addition, the adhesion strength of the coatings was measured according to the attachment and removing a pressure-sensitive tape, based on the American Standard Test Method (ASTM) D3359. The adhesion strength was rated in the scale of 0-5B.

The corrosion resistance of the various nanocomposite coatings was considered by potentiodynamic polarization test (PARSTAT2273, AMETEK) in simulated body fluid (SBF) at the scanning rate of 1 mV/s and the potential range of ± 0.5 V vs. open circuit potential (OCP). Initially, the samples were immersed in SBF for 1 h to reach an equilibrium state. The applied electrochemical cell consisted of the sample as the cathode, Ag/AgCl reference electrodes and a platinum sheet as anode. Potentiodynamic polarization test was performed in the potential range of ± 0.5 V vs. open circuit potential (OCP).

2.6. Antibacterial Test

The antibacterial activity test was carried out using *Escherichia coli* (*E. coli*) as Gram-negative bacteria and *Staphylococcus aureus* (*S. aureus*) as Gram-positive bacteria. Bacterial culture process was performed via incubation in a broth medium containing meat extract (0.5 g), NaCl (0.5 g) and peptone (1.0 g) dissolved in distilled water (100 ml, pH ≃ 7.2) at 37 °C for 24 h. Subsequently, the bacterial population (10^7 CFU/ml) was diluted to 10^5 CFU/ml. All specimens were cleaned with ethanol and then transferred to a sterilized 24-well plate, followed by addition of 1 ml bacterial culture onto their surface. The samples were then kept at 37 °C for 18 h. Bacterial culture was diluted 100 × via phosphate buffer solution (PBS, pH ≃ 7.1). Afterwards, bacterial count in each well was determined by the pour plate method on Nutrient Agar at 37 °C for 24 h. Antibacterial rate (%) was calculated according to Eq. (1) [30].

$$\text{Antibacterial rate (\%)} = \frac{(N_U - N_C)}{N_U} \times 100 \quad (1)$$

where N_U is bacterial count on uncoated specimens after incubation and N_C is bacterial count on coated specimens after incubation.

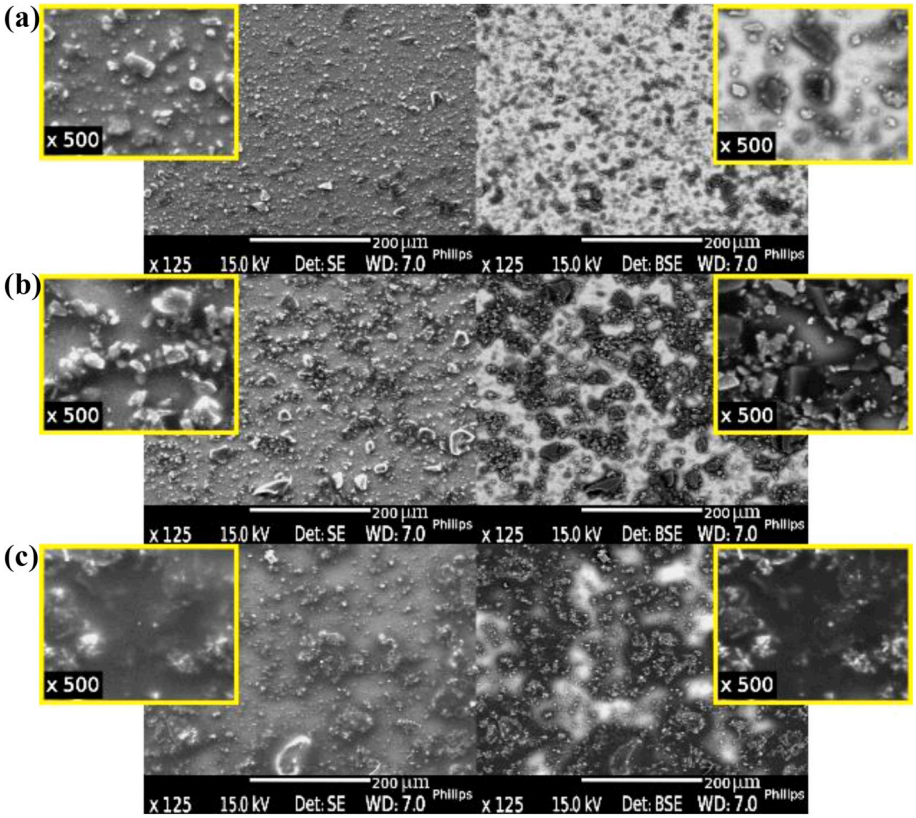

Fig. 3. SEM micrographs of nanocomposite coatings consisting of various amounts of CuO-NPs at two different magnifications (125× and 500×) and imaging modes (back scatter and secondary electron scatter modes): a) PDMS-SiO_2–0.5 wt% CuO (PSC0.5), b) PDMS-SiO_2–1 wt% CuO (PSC1) and (c) PDMS-SiO_2–2 wt% CuO (PSC2).

2.7. Cell Culture

Cytotoxicity of the coatings was evaluated using culture of MG63 cell-line purchased from Royan Institute of Iran. Before cell seeding, MG63 cells were incubated in full culture medium consisting of Dulbecco's Modified Eagle Medium (DMEM-low, Bioidea, Iran) supplemented with 10% (*v*/v) fetal bovine serum (FBS, Bioidea, Iran) and 1% (v/v) streptomycin/penicillin (Bioidea, Iran) at 37 °C and 5% CO_2 environmental condition. In another word, the coated samples were rinsed with PBS (Bioidea, Iran) and, consequently, sterilized in ethanol (1 h) followed by exposure to UV light (6 h). Finally, MG63 cells with a density of 10^4 cells/well were seeded on the samples and tissue culture plate (TCP) as the control ($n = 3$) and were incubated for the specific time points.

The viability of cells seeded on the samples was studied by MTT assay, which was performed according to manufacturer's protocol (Sigma). At the specific time points (1, 3 and 7 days), the cell-seeded samples were incubated with MTT solution (0.5 g/ml in PBS) for 4 h. Finally, the optical density (OD) of formazan solution in DMSO (Merck) was determined using a microplate reader (Biotech) at a wavelength of 490 nm, against DMSO (blank). Finally, the viability of cells, compared to control, was calculated according to the following Eq. (2) [31]:

$$\text{Relative cell survival (\%control)}: \frac{A_{Sample} - A_b}{A_c - A_b} \quad (2)$$

in which A_{Sample}, A_b and A_c are the absorbance value of the sample, DMSO and control (TCP), respectively.

In addition, the spreading of cells cultured on the coated samples was considered by SEM technique. The cell-seeded samples were fixed with 2.5% glutaraldehyde (Sigma) solution in PBS for 3 h. After two-time rinsing with PBS, the fixed samples were dehydrated in the graded concentrations of ethanol (30–100% (*v*/v)), respectively. Finally, the samples were dried up in the air, gold coated and finally assessed using SEM.

2.8. Statistical Analysis

The biological data was statistically examined via one-way ANOVA analysis to assess the significant difference. The statistical significance between the groups was studied using Tukey-Kramer post-hoc test using GraphPad Prism Software (V.6). In this study, *P*-value < .05 was defined as statistically significant.

3. Results and Discussion

3.1. Characterization of Nanocomposite Coatings

Before nanocomposite coating process, CuO and SiO_2 nanopowders were synthesized, separately. XRD pattern of CuO (Fig. 2(a)) consisted of two sharp peaks at 2θ = 35.7° and 38.8° corresponded to (002) and (111) crystallographic planes, respectively. In addition, there were other noticeable peaks at 2θ = 48°, 53° and 58° related to the ($\bar{2}02$), (020) and (202) planes, respectably. Results indicated that pure CuO nanoparticles were synthesized and the secondary phase of $Cu(OH)_2$ was not detected in powder. It was suggested that CuO was completely synthesized based on reaction (1) [32]:

$$CuCl_2 + 2NaOH \rightarrow Cu(OH)_2 + 2NaCl \rightarrow CuO + H_2O \quad \text{(Reaction 1)}$$

Moreover, the crystallite size of CuO nanoparticles measured by Scherer equation was determined 23 ± 5 nm. In addition, the average particle size of CuO measured using DLS test (Fig. 2(b)) was estimated about 200 nm. According to SEM images, CuO nanoparticles (Fig. 2(c)) consisted of rod shaped morphology with approximately similar size. This morphology might provide appropriate surface to contact with bacteria sufficiently [33,34].

In addition to CuO, SiO_2 nanopowder were synthesized via sol-gel process. No considerable peak could be detected in XRD pattern of SiO_2 powder proving the amorphous nature of silica (Fig. 2(d)). However,

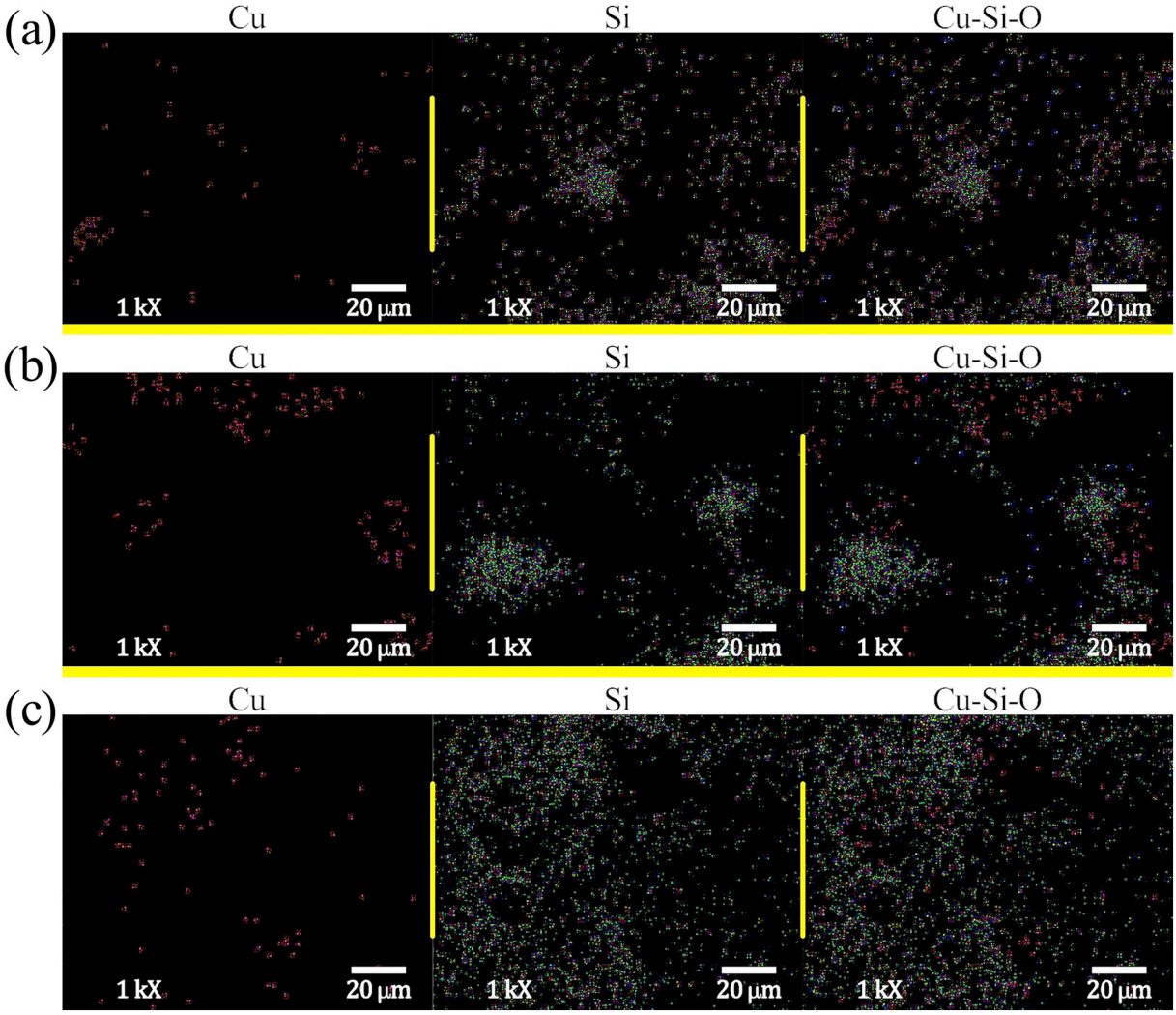

Fig. 4. Elemental mapping analysis of nanocomposite coatings consisting of various amounts of CuO contents: a) 0.5 wt% (PSC0.5), b) 1 wt% (PSC1) and c) 2 wt% (PSC2). Cu (pink), Si (green) and O (yellow). (For interpretation of the references to color in this figure legend, the reader is referred to the web version of this article.)

FTIR spectrum of silica nanopowder (Fig. 2(e)) confirmed the formation SiO_2 without the presence of any organic precursors. At 1010–1055 cm^{-1}, the Si − O − Si symmetric stretching vibration mode could be detected. Moreover, two characteristic peaks at 1257 and 790 cm^{-1} were detected which were corresponded to Si − CH_3 bonds of silica based material. Symmetric and asymmetric stretching mode of C − H bond was also detected at 2962 cm^{-1} showing epoxy groups. Moreover, SEM image of SiO_2 (Fig. 2(f)) shows the formation of semi-spherical and irregular particles with large agglomerates in the range of 6 ± 2 µm.

XRD pattern of PDMS-SiO_2–2 wt% CuO(PSC2) nanocomposite coating (Fig. 2(g)) showed the presence of sharp peak at $2\theta = 44.6^{\circ}$ related to (100) plane of 316 L stainless steel [35]. Additionally, two peaks of CuO nanoparticles were detected implying the presence of nanocomposite coating on the stainless steel. Moreover, there was no sharp peak relating to PDMS and silica in the XRD pattern due to the amorphous nature of these materials [34]. Additionally, the chemical composition of PDMS, PDMS-SiO_2 (PS) and PSC2 coatings was investigated by FTIR spectroscopy (Fig. 2(h)). FTIR spectrum of PDMS coating consisted of the characteristic band at 1031–1089 cm^{-1} corresponded to the symmetric stretching vibration of Si − O − Si indicating the presence of a network structure inside the coatings [36]. Two characteristic sharp peaks observed at 790–802 cm^{-1} and 1260 cm^{-1} represented the Si − CH_3 symmetric deformation of PDMS. A peak observed at 1400 cm^{-1} indicated symmetric deformation vibration of Si−phenyl bonds. The absorption band was detected at 2960 cm^{-1} relating to asymmetric stretching vibration band of C − H bonds. This peak was considered to be either from residual epoxy groups because of partial hydrolysis and/or the formation of methyl groups at sol–gel synthetize process [37]. FTIR spectrum of PS coating consisted of Si − O − Si symmetric stretching vibration and Si − CH_3 symmetric deformation of PDMS. Moreover, the broad stretching band at 3435 cm^{-1} and the weak deformation vibration band of −OH group at 1600–1630 cm^{-1} in the spectrum, indicating a small amount of hydroxyl groups in PS coating. After incorporation of CuO within nanocomposite coating (PSC2), the intensity of C − H bonds and Si−phenyl bonds increased and the intensity of −OH bonds decreased which could be helpful for improved super-hydrophobicity of the coatings [37,38].

SEM micrographs of PSC0.5, PSC1 and PSC2 nanocomposite coatings at two different imaging modes (secondary and backscattered electron imaging) are depicted in Fig. 3. The micrographs consisted of small irregular-shape particles with size of 3.5 ± 1.5 µm referring to monoclinic structure of CuO and relatively large agglomerated SiO_2 particles with irregular shapes referring to monoclinic structure of CuO. This morphology could be clearly detected at backscattered electron images. Moreover, increasing amounts of CuO nanoparticles changed

Table 1
Roughness, contact angle and surface adhesion of PDMS, PS and PSC nanocomposite coated 316 L SS.

Sample name	Roughness Ra (μm)	Contact angle (°)	Drop figure	Area removed %	Classification	ASTM D3359 pattern
PDMS	0.07 ± 0.01	74 ± 4		5	4B	
PS	1.39 ± 0.12	89 ± 5		50	1B	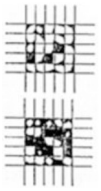
PSC0.5	1.14 ± 0.01	88 ± 8	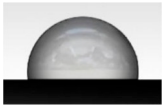	15	3B	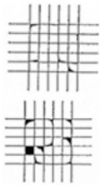
PSC1	2.49 ± 0.04	146 ± 6	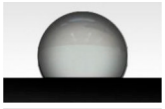	75	0B	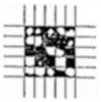
PSC2	2.21 ± 0.09	142 ± 8	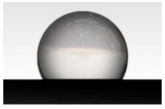	50	1B	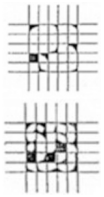

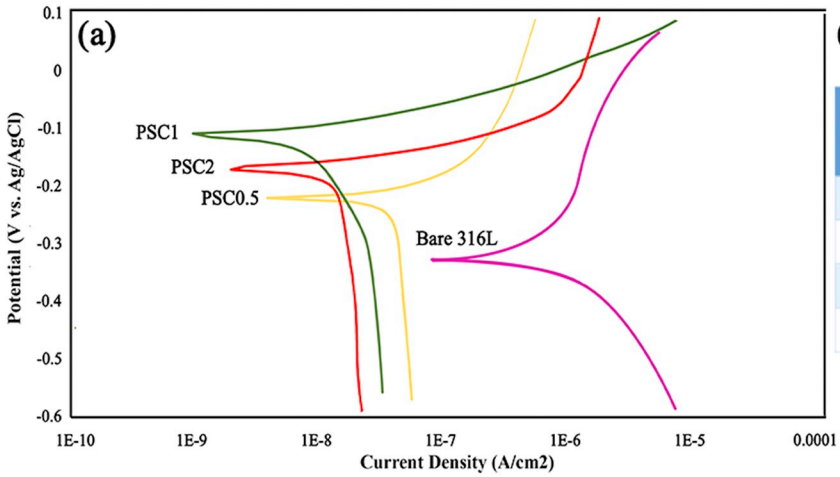

(b)

Sample	Current density (A/cm^2)	Potential (V)
Bare 316L	6.2E-7	-0.33
PSC0.5	5.1E-8	-0.21
PSC1	8.1E-9	-0.10
PSC2	1.3E-8	-0.18

Fig. 5. Corrosion behavior of the nanocomposite coatings consisting various amounts of CuO-NPs as well as 316L substrate: Potentiodynamic polarization curves and b) the analysis data extracted from potentiodynamic polarization curves of nanocomposite coatings consisting of 0.5 wt% CuO (PSC0.5), 1 wt% CuO (PSC1) and 2 wt % CuO (PSC2).

the surface smoothness and provided the rough surface. EDS analysis (Fig. 4) revealed different dispersions of CuO nanoparticles on the surface, depending on the CuO concentration. While the powder scattered homogeneously on the surface of at PSC0.5 and PSC1 coatings, the agglomerated CuO nanoparticles found on the PSC2 sample.

One of the most important properties of coatings affecting their antibacterial, cell function and wettability is surface roughness. Therefore, the average roughness of various nanocomposite coatings consisting of various amounts of CuO nanoparticles were estimated (Table 1). Results showed that, presence of silica and CuO nanoparticles significantly improved surface roughness. For example, the surface roughness enhanced (1.4 times) from 0.07 ± 0.01 μm (at PDMS) to 2.49 ± 0.04 μm (at PSC1). By increasing CuO nanoparticle concentration, the PDMS chains could not bind all nanoparticles. Hence, there was a number of unbounded nanoparticles sticking out of the surface resulted in enhanced surface roughness. However, more increasing the CuO nanoparticles did not significantly change the surface roughness ($P > 0.05$). It might be due to agglomeration of nanoparticles in the PSC2 sample [39]. Moreover, in order to evaluate hydrophobicity of coatings, the contact angle of water drop was measured

Table 2
Antibacterial rate of coated specimens consisting different amounts of CuO nanoparticles against two types of positive and negative bacterial (*Staphylococcus aureus* and *Escherichia coli*).

Sample name	Antibacterial rate (%)	
	E. coli	*S. aureus*
PS	0.00	00
PSC0.5	92.69	75.14
PSC1	90.14	69.55
PSC2	78.27	65.36

(Table 1). Our results showed that, PDMS coating enhanced the water contact angle of stainless steel from 70 ± 1° to 74 ± 4° relating to the hydrophobic nature of PDMS [40]. However, water contact angle reported for PDMS was often 100 ± 5°. Less hydrophobicity of pure PDMS in this research was related to substrate modification by acid leading to formation of –OH groups and enhanced surface roughness. This behavior was similarly reported in previous researches and water contact angel of PDMS was reported around 70.6 ± 4.2° [41]. Moreover, incorporation of silica nanoparticles promoted hydrophobicity to 89 ± 5°. Furthermore, the contact angle significantly enhanced to 142 ± 8° by increasing CuO content upon 2 wt% ($P < 0.05$) which might be related to the surface roughness of samples. Among the samples, PSC1 revealed the greatest hydrophobicity (contact angle = 146 ± 8°) [20]. This behavior was similarly reported in previous researches [16,42]. For instance, Tang et al. [42] similarly proved that surface roughness affected hydrophobicity performance, antibacterial activity and bacteria adhesion. Presence of a dual-scale roughness (micro- and nano-scale) resulted in formation of a lotus leaf structure which enhanced hydrophobic characterize of the coating [16,43].

Adhesion resistivity of the coating is a critical property to reach mechanical integrity [44]. Adhesion strength of PDMS, PS and PSC nanocomposite coatings were investigated based on ASTM D3359 protocol. Our result showed that PDMS coating adhered vigorously to stainless steel substrate and adhesion strength was estimated about 4B. It might be due to silane groups which chemically bounded to the stainless steel [45]. After incorporation of SiO_2 in the PDMS coating (PS), despite the strong (Si-O-Si) interaction between PDMS and SiO_2 nanoparticles, due to poor linking between SiO_2 and stainless steel, around 50% of coating was peeled off making it unsuitable for coating application [46]. Among various nanocomposite coatings, PSC0.5 revealed the highest adhesion strength which was nearly close to that of PDMS coating. More incorporation of CuO nanoparticles resulted in the significant reduction in the silane groups on the surface leading to poor adhesion of coating to the substrate.

Fig. 5(a) shows Tafel polarization curves of stainless steel 316 L and the nanocomposite coated samples in SBF solution at pH = 7.4 at room temperature. Furthermore, the extracted electrochemical parameters including the corrosion potential (E_{corr}) and the current density (i_{corr}) are provided in Fig. 5(b). Overall, results showed that, the E_{corr} values of all nanocomposite coated samples were more positive than that of 316 L stainless steel substrate. Therefore, the PDMS-SiO_2-CuO coatings acted as a corrosion-resistant barrier. Moreover, the i_{corr} values of all coated samples were dramatically lower than that of the uncoated

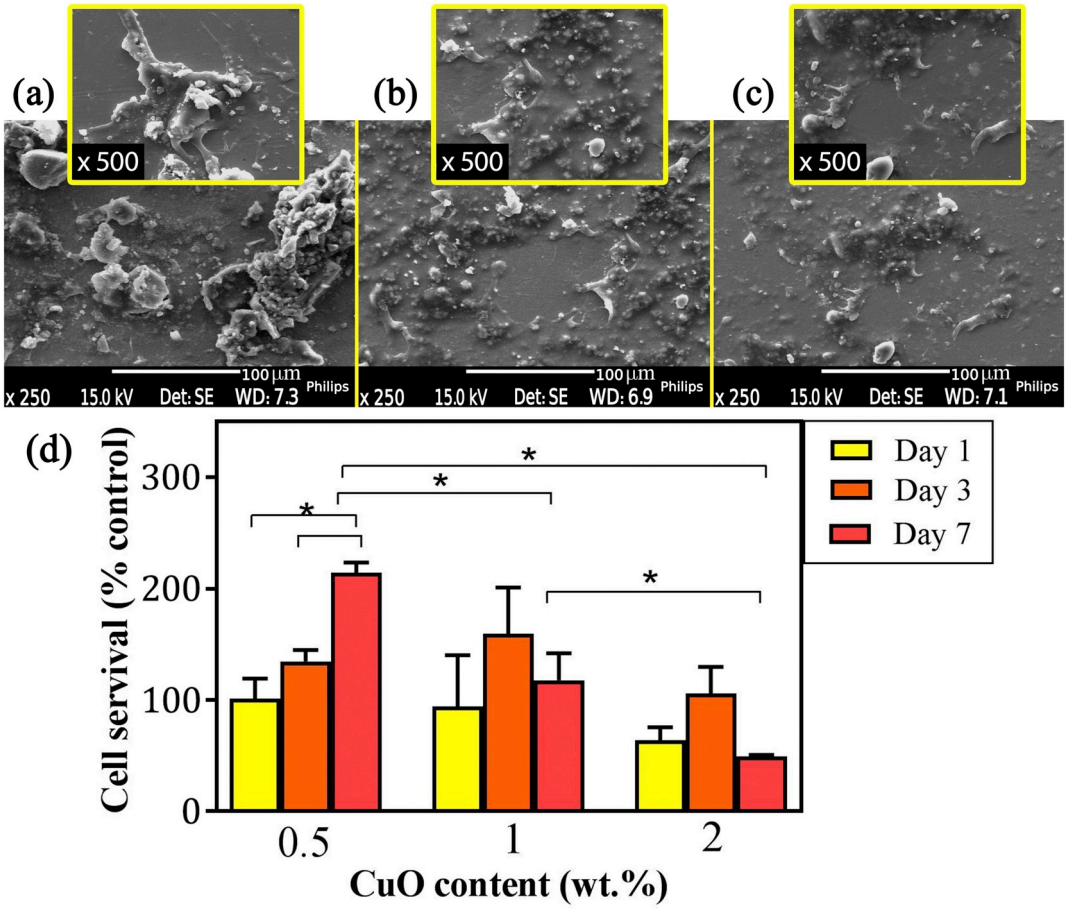

Fig. 6. Biological properties of the nanocomposite coatings: SEM images of MG63 cell-seeded samples after 7 days of culture at two different magnifications: a) 0.5 wt % (PSC0.5), b) 1 wt% (PSC1) and c) 2 wt% (PSC2). d) Cell viability evaluation of MG63 seeded on the nanocomposite coatings consisting of various amounts of CuO nanoparticles using MTT assays, after 1, 3 and 7 days of culture. The absorbance was normalized against the control (TCP) at each time interval. (*$P < 0.05$).

sample, confirming that the presence of the PDMS-SiO_2-CuO coatings could reduce the corrosion attack. However, depending on the CuO content in the coatings, the anti-corrosion resistant property was different. For instance, increasing the concentration of CuO to 1 wt% (PSC1) resulted in a significant reduction of the i_{corr} values. Firstly, incorporation of CuO nanoparticles with hydrophobic nature and dielectric construction, could create a denser structure of coating and restrict ion diffusion through the surface. Consequently, the electrochemical reactions in the electrolyte and on the surface of samples diminished, significantly. Hence, PSC1 was the most resistant to the SBF solution. This result was compatible with water contact angle data. Second perspective which could be considered, is roughness. Surface roughness could substantially affect the corrosion behavior of the coatings [12]. According to Table 1, incorporation of CuO nanoparticles enhanced the surface roughness from 1.14 to 2.49 μm. Therefore, air molecules could be entrapped into surface pores leading to surface protection from corrosive environment. Incorporation of more CuO nanoparticles led to increase in the i_{corr} values due to the agglomeration of CuO nanoparticles resulted in the formation of a micro-pores on the surface. This morphology resulted in the penetration of the corroded solution into the coating and reaching it to the coating/substrate interface to increase the corrosion. Therefore, PSC1 with the highest hydrophobicity and roughness revealed the best corrosion resistance.

3.2. Antibacterial Activity Test

Antibacterial activity of the coatings against two types of positive and negative bacterial (*Staphylococcus aureus* and *Escherichia coli*) was evaluated and presented at Table 2. Our results revealed that, PS coating did not show any antibacterial characteristic (antibacterial rate = 0%), confirming the significant role of CuO nanoparticles to kill the bacteria. Moreover, the antibacterial activity of the nanocomposite coated specimens consisting of various amounts of CuO nanoparticles was much better against *E. coli* than that of *S. aureus* which might be due antibacterial activity of CuO nanoparticles against positive and negative gram bacterials. Similarly, Dan et al. [30] showed that the important factor in antibacterial activity of CuO nanoparticles was their penetration feasibility into the cell membrane which depended on the thickness of peptidoglycan in bacterial cell wall. While the peptidoglycan thickness in Gram-positive bacteria is 10–100 nm, it is 2–3 nm at in Gram-negative bacteria. Therefore, it would be difficult for CuO nanoparticles to penetrate into the cell membrane of *S. aureus* as the Gram-positive bacteria. On the other side, increasing the concentration of CuO nanoparticles from 0.5 to 2.0 wt% resulted in reduced antibacterial effect for both groups of bacterial. The high antibacterial rate of 92.69% and 90.14% against *E. coli* were monitored by using 0.5 and 1 wt% of CuO nanoparticles, respectively. The PSC0.5 showed the highest antibacterial rate of 75.14% against *S. aureus*. In the terms of the antibacterial effect of nanoparticles, they should diffuse to the bacterial solution to kill the bacteria [47]. According to the SEM micrographs, CuO nanoparticles were more agglomerated by increasing their content leading to less diffusivity of the nanoparticles at 2 wt% concentration and subsequently lower antibacterial rate.

3.3. Cell Morphology and Proliferation

Despite the effective role of CuO nanoparticles on the antibcterial characteristics of nanocomposite coatings, it might have reverse role on the cell function. Therefore, the optimized concentration of CuO nanoparticles based on the cytotoxicity evaluation is crucial. In this way, the morphology of cells is a critical parameter to evaluate the cell-biomaterial interaction. SEM images of cell seeded samples after 7 days of culture are presented in Fig. 6(a-c). Results showed that MG63 cells covered more area of PSC0.5, while a limited number of cells were attached on the surface of PSC2. Moreover, MTT assay was done to study the viability of cells. Fig. 6(d) shows that viability of cells seeded on PSC0.5 considerably improved from day 1 (100 ± 18 (%control)) to day 7 (200 ± 9.4 (%control)) ($P < 0.05$). However, incorporation of more CuO nanoparticles within the coatings resulted in reduced cell survival from day 3 to day 7 of culture. For example, the proliferation of cells seeded on the PSC1 sample increased from 94 ± 36 (% control) (at day 1) to 159 ± 41 (%control) (at day 3) and consequently reduced to 117 ± 24 (% control) after 7 days of culture. Moreover, the MTT assay revealed that the proliferation of MG63 cells reduced with increasing CuO content in the coating. Noticeably, after 7 days, while the proliferation of cells on the PSC0.5 sample was 200 ± 9.4 (%control), it was reduced to 49 ± 1.7 (% control) on PSC2 sample ($P < .05$). However, compared to control (tissue culture plate), the proliferation of MG63 cells on the PSC2 sample was significantly reduced confirming the role of CuO incorporated in the coatings. In conclusion, we demonstrated that hybrid PSC0.5 coating could highly promote MG63 cell adhesion, spreading, and proliferation making it suitable for biomedical implants.

4. Conclusion

In this present study, PDMS-SiO_2-CuO nanocomposite coatings consisting of various amounts of CuO nanoparticles were developed. While PDMS coating with high adhesive strength was hydrophobic (74 ± 4°), incorporation of CuO nanoparticles within PDMS-SiO_2 coatings significantly promoted hydrophobic property of the coating and improved surface roughness leading to noticeably enhanced corrosion resistance. Thanks to antibacterial characteristic of CuO nanoparticles as well as improved hydrophobic property of the coatings, incorporation of CuO nanoparticles within the coatings significantly enhanced antibacterial rate of nanocomposite coatings compared to PDMS-SiO_2 coating. However, incorporation of CuO nanoparticles > 0.5 wt% resulted in reduced antibacterial characteristic of the coatings due to the agglomeration of the nanoparticles. Moreover, MG63 cells attached, spread and proliferated on the various nanocomposite coatings depending on the CuO content. Our results confirmed that PDMS-SiO_2-CuO nanocomposite coating consisting of 0.5 wt% CuO significantly improved cell proliferation. In summary, we demonstrated that the PDMS-SiO_2-CuO nanocomposite coating with significant antibacterial and anticorrosion behavior and appropriate biocompatibility has great potential for the temporary implants applied for bone repair.

References

[1] F. Witte, The history of biodegradable magnesium implants: a review, Acta Biomater. 6 (5) (2010) 1680–1692.
[2] C. Garcia, S. Cere, A. Duran, Bioactive coatings prepared by sol–gel on stainless steel 316L, J. Non-Cryst. Solids 348 (2004) 218–224.
[3] D.-M. Liu, Q. Yang, T. Troczynski, Sol–gel hydroxyapatite coatings on stainless steel substrates, Biomaterials 23 (3) (2002) 691–698.
[4] M.H. Fathi, et al., In vitro corrosion behavior of bioceramic, metallic, and bioceramic–metallic coated stainless steel dental implants, Dent. Mater. 19 (3) (2003) 188–198.
[5] R. Tracana, J. Sousa, G. Carvalho, Mouse inflammatory response to stainless steel corrosion products, J. Mater. Sci. Mater. Med. 5 (9–10) (1994) 596–600.
[6] R. Tracana, et al., Stainless steel corrosion products cause alterations on mouse spleen cellular populations, J. Mater. Sci. Mater. Med. 6 (1) (1995) 56–61.
[7] S. Morais, et al., Decreased consumption of Ca and P during in vitro biomineralization and biologically induced deposition of Ni and Cr in presence of stainless steel corrosion products, J. Biomed. Mater. Res. 42 (2) (1998) 199–212.
[8] L. Zhao, et al., Antibacterial coatings on titanium implants, J. Biomed. Mater. Res. B Appl. Biomater. 91 (1) (2009) 470–480.
[9] Z.X. Voo, et al., Antimicrobial/antifouling polycarbonate coatings: role of block copolymer architecture, Macromolecules 48 (4) (2015) 1055–1064.
[10] J. Bumgardner, et al., Contact angle, protein adsorption and osteoblast precursor cell attachment to chitosan coatings bonded to titanium, J. Biomater. Sci. Polym. Ed. 14 (12) (2003) 1401–1409.
[11] S. Pinto, et al., Poly (dimethyl siloxane) surface modification by low pressure plasma to improve its characteristics towards biomedical applications, Colloids Surf. B: Biointerfaces 81 (1) (2010) 20–26.
[12] M. Jokar, et al., Corrosion and bioactivity evaluation of nanocomposite PCL-forsterite coating applied on 316L stainless steel, Surf. Coat. Technol. 307: p (2016) 324–331.

[13] R. Torkaman, et al., Electrochemical and in vitro bioactivity of nanocomposite gelatin-forsterite coatings on AISI 316 L stainless steel, Prog. Org. Coat. 103 (2017) 40–47.
[14] A. Mata, A.J. Fleischman, S. Roy, Characterization of polydimethylsiloxane (PDMS) properties for biomedical micro/nanosystems, Biomed. Microdevices 7 (4) (2005) 281–293.
[15] S. Flint, J. Brooks, P. Bremer, Properties of the stainless steel substrate, influencing the adhesion of thermo-resistant streptococci, J. Food Eng. 43 (4) (2000) 235–242.
[16] X. Liu, et al., Super-hydrophobic property of nano-sized cupric oxide films, Surf. Coat. Technol. 204 (20) (2010) 3200–3204.
[17] A. Tserepi, M. Vlachopoulou, E. Gogolides, Nanotexturing of poly (dimethylsiloxane) in plasmas for creating robust super-hydrophobic surfaces, Nanotechnology 17 (15) (2006) 3977.
[18] R. Allaker, The use of nanoparticles to control oral biofilm formation, J. Dent. Res. 89 (11) (2010) 1175–1186.
[19] D. Vasconcelos, et al., Corrosion resistance of stainless steel coated with sol–gel silica, J. Non-Cryst. Solids 273 (1–3) (2000) 135–139.
[20] W. Ming, et al., Superhydrophobic films from raspberry-like particles, Nano Lett. 5 (11) (2005) 2298–2301.
[21] E.J. Park, et al., Transparent and superhydrophobic films prepared with polydimethylsiloxane-coated silica nanoparticles, RSC Adv. 3 (31) (2013) 12571–12576.
[22] J. Xie, et al., Robust and anti-corrosive PDMS/SiO_2 superhydrophobic coatings fabricated on magnesium alloys with different-sized SiO_2 nanoparticles, Appl. Surf. Sci. 457 (2018) 870–880.
[23] P. de Lima Neto, et al., Sol-gel ZrO2 coatings for chemical protection of stainless steel, J. Sol-Gel Sci. Technol. 1 (2) (1994) 177–184.
[24] M. Michał, et al., The newest achievements in synthesis, immobilization and practical applications of antibacterial nanoparticles, Chem. Eng. J. 228 (2013) 596–613.
[25] M. Atik, et al., Protection of 316L stainless steel against corrosion by SiO_2 coatings, J. Mater. Sci. Lett. 13 (15) (1994) 1081–1085.
[26] G. Ren, et al., Characterisation of copper oxide nanoparticles for antimicrobial applications, Int. J. Antimicrob. Agents 33 (6) (2009) 587–590.
[27] G. Cindy, et al., Cytotoxic origin of copper(II) oxide nanoparticles: Comparative studies with micron-sized particles, leachate, and metal salts, ACS Nano 5 (9) (2011) 7214–7225.
[28] H. Pang, F. Gao, Q. Lu, Morphology effect on antibacterial activity of cuprous oxide, Chem. Commun. (9) (2009) 1076–1078.
[29] K.S. Rao, et al., A novel method for synthesis of silica nanoparticles, J. Colloid Interface Sci. 289 (1) (2005) 125–131.
[30] Z. Dan, et al., Microstructure and antibacterial properties of AISI 420 stainless steel implanted by copper ions, Thin Solid Films 492 (1–2) (2005) 93–100.
[31] N. Golafshan, M. Kharaziha, M. Fathi, Tough and conductive hybrid graphene-PVA: Alginate fibrous scaffolds for engineering neural construct, Carbon 111 (2017) 752–763.
[32] S. Sonia, et al., Effect of NaOH concentration on structural, surface and antibacterial activity of CuO nanorods synthesized by direct sonochemical method, Superlattice. Microst. 66 (2014) 1–9.
[33] X. Wang, et al., Shape-dependent antibacterial activities of Ag_2O polyhedral particles, Langmuir 26 (4) (2009) 2774–2778.
[34] N. Talebian, S.M. Amininezhad, M. Doudi, Controllable synthesis of ZnO nanoparticles and their morphology-dependent antibacterial and optical properties, J. Photochem. Photobiol. B Biol. 120 (2013) 66–73.
[35] E. Barrera-Calva, et al., Silica-copper oxide composite thin films as solar selective coatings prepared by dipping sol gel, Adv. Mater. Sci. Eng. 2008 (2008).
[36] S.D. Burnside, E.P. Giannelis, Synthesis and properties of new poly (dimethylsiloxane) nanocomposites, Chem. Mater. 7 (9) (1995) 1597–1600.
[37] A.V. Rao, et al., Water repellent porous silica films by sol–gel dip coating method, J. Colloid Interface Sci. 352 (1) (2010) 30–35.
[38] S.A. Mahadik, et al., Superhydrophobic silica coating by dip coating method, Appl. Surf. Sci. 277 (2013) 67–72.
[39] R. Zarzuela, et al., CuO/SiO2 nanocomposites: a multifunctional coating for application on building stone, Mater. Des. 114 (2017) 364–372.
[40] C. Kapridaki, P. Maravelaki-Kalaitzaki, TiO2–SiO2–PDMS nano-composite hydrophobic coating with self-cleaning properties for marble protection, Prog. Org. Coat. 76 (2–3) (2013) 400–410.
[41] K. Chan, et al., The surface modification of stainless steel and the correlation between the surface properties and protein adsorption, J. Mater. Sci. Mater. Med. 18 (7) (2007) 1389–1398.
[42] H. Tang, et al., Influence of silicone surface roughness and hydrophobicity on adhesion and colonization of Staphylococcus epidermidis, J. Biomed. Mater. Res. A 88 (2) (2009) 454–463.
[43] W. Barthlott, C. Neinhuis, Purity of the sacred lotus, or escape from contamination in biological surfaces, Planta 202 (1) (1997) 1–8.
[44] Z. Chen, et al., A review on the mechanical methods for evaluating coating adhesion, Acta Mech. 225 (2) (2014) 431–452.
[45] L.B. Boinovich, et al., Durable icephobic coating for stainless steel, ACS Appl. Mater. Interfaces 5 (7) (2013) 2549–2554.
[46] L. Kersey, et al., The effect of adhesion promoter on the adhesion of PDMS to different substrate materials, Lab Chip 9 (7) (2009) 1002–1004.
[47] M. Li, et al., Antibacterial performance of a Cu-bearing stainless steel against microorganisms in tap water, J. Mater. Sci. Technol. 31 (3) (2015) 243–251.